Textural Properties of Porous Solids in Relation to Gas Transport

O. ŠOLCOVÁ, H. ŠNAJDAUFOVÁ, V. HEJTMÁNEK, and P. SCHNEIDER

Institute of Chemical Process Fundamentals, Academy of Sciences of the Czech Republic, CZ-165 02 Prague

Received 14 June 1999

The aim of this study is to compare pore structure characteristics of two industrial catalysts determined by standard methods of textural analysis (physical adsorption of nitrogen and mercury porosimetry) and selected methods for obtaining parameters relevant to transport processes (multicomponent diffusion and permeation of gases). The Mean Transport Pore Model (MTPM) described diffusion and permeation and the Dusty Gas Model (DGM) described permeation; models (represented as a boundary value problem for a set of ordinary differential equations) are based on Maxwell—Stefan diffusion equation and Weber permeation law. Parameters of models are material constants of the porous solid and, thus, do not depend on conditions under which the transport processes take place. Both catalysts were mono- or bidispersed with mean pore radii about 70 nm and 2000 nm; diffusion and permeation measurements were performed with four inert gases (H_2, He, N_2, and Ar).

The industrial application of porous solids is quite widespread. Porous heterogeneous catalysts, adsorbents, and membranes are used in chemical industry and in biotechnology, porous materials are common in building engineering, porous catalysts form the basis of car mufflers, *etc.* The rates of processes, which take place in pore structure of these materials, are affected or determined by the transport resistance of the pore structure. Inclusion of transport processes into the description of the whole process is essential when reliable simulations or predictions have to be made. Trends in modern chemical/biochemical reaction engineering point to utilization of more sophisticated, and therefore more reliable, models of processes. The basic idea is that the better the description of individual steps of the whole process the better its description and, perhaps, even extrapolation.

Because of the unique nature of pore structure of different materials the pore structure characteristics relevant to transport in pores have to be determined experimentally. Two approaches are used in this respect:

- textural analysis of the porous solid;
- evaluation of simple transport processes taking place in the porous solid in question.

The advantage of the first approach derives from the complexity of available experimental methods and evaluation procedures (physical adsorption of gases, high-pressure mercury porosimetry, liquid expulsion permporometry, permporometry with pores blocked by capillary condensation, *etc.*).

The relevance of the second approach stems from the possibility to use the same pore-structure model as used in description of the process in question (countercurrent (isobaric) diffusion of simple gases, permeation of simple gases under steady-state or dynamic conditions, combined diffusion and permeation of gases under dynamic conditions, *etc.*).

THEORETICAL

Transport parameters, *i.e.* model parameters that are material constants of the porous solids (independent of temperature, pressure, and kind and concentration of gases) are evaluated through application of a suitable model of porous solids to results of measurements of simple transport processes in the porous structure. Today only two models are available for description of combined (diffusion and permeation) transport of multicomponent gas mixtures: the Mean Transport Pore Model (MTPM) [1, 2] and the Dusty Gas Model (DGM) [3, 4]. Both models are based on the modified Stefan—Maxwell description of multicomponent diffusion in pores and on Darcy (DGM) or Weber (MTPM) equation for permeation. For mass transport due to composition differences (*i.e.* pure diffusion) both models are represented by an identical set of differential equations with two parameters (transport parameters) which characterize the pore structure. Because both models drastically simplify the real pore structure, the transport parameters have to be determined experimentally.

MTPM assumes that the decisive part of the gas transport takes place in transport pores that are visualized as cylindrical capillaries with radii distributed around the mean value $\langle r \rangle$ (first model parameter).

The second model parameter can be looked upon as ratio of tortuosity, q_t, and porosity of transport pores, ε_t, $\psi = \varepsilon_t/q_t$. The third transport parameter, $\langle r^2 \rangle$ [5], characterizes the width of the transport pore size distribution and is required for description of viscous flow in pores.

DGM visualizes the porous medium as a collection of giant spherical molecules (dust particles) kept in space by external force. The movement of gas molecules in the space between dust particles is described by the kinetic theory of gases. Formally, the MTPM transport parameters $\langle r \rangle$ and ψ can be used also in DGM. The third DGM transport parameter characterizes the viscous (Poiseuille) gas flow in pores.

The Dusty Gas Model (DGM) and Mean Transport Pore Model (MTPM) are based on the Maxwell—Stefan theory. Both models include contributions of bulk diffusion, Knudsen diffusion, and permeation flow that accounts both for viscous flow and Knudsen flow (MTPM includes also the slip at the pore wall). The vector form of the relation between molar flux densities, $\boldsymbol{N} = \{N_1, N_2, \ldots, N_n\}^T$, and gradients of molar concentrations, $\boldsymbol{c} = \{c_1, c_2, \ldots, c_n\}^T$, is the same for both models

$$\mathbf{H}(\boldsymbol{c}) \quad \boldsymbol{N} + \frac{\partial \boldsymbol{c}}{\partial x} = 0 \qquad (1)$$

where $\mathbf{H}(\boldsymbol{c})$ is a square $(n*n)$ concentration-dependent matrix (for matrix elements, h_{ij}, see Appendix). This matrix hides [6] the differences between both models. The matrix elements depend on transport properties of pure gases and their binary mixtures, and on the structure of the porous solid (characterized by three parameters ψ, $\langle r \rangle \psi$, and $\langle r^2 \rangle \psi$).

The best way for obtaining transport parameters of porous structures is to follow experimentally a simple transport processes in the pores under uncomplicated process conditions (temperature, pressure, *etc.*) and to evaluate the model parameters by fitting the obtained experimental results to the theory.

The experimentally performed transport processes used for evaluation of transport parameters include: counter-current binary or multicomponent gas diffusion under steady-state or chromatographic conditions, steady permeation of simple gases, dynamics of combined transport of binary or multicomponent gas mixtures, *etc.* Of significance, however, is that no automatic commercial instrument is available for these processes. Thus, the necessary apparatuses must be home-made. To obtain the transport parameters with acceptable confidence large number of experiments is required. It would be, therefore, of significant importance if at least part of the transport parameters could be obtained from standard textural analysis.

The aim of this study is to compare pore structure characteristics of two porous catalysts determined by standard methods of textural analysis (physical adsorption of nitrogen and mercury porosimetry) and selected methods for obtaining parameters relevant to transport processes (multicomponent gas diffusion and permeation of simple gases). MTPM was used for description of both processes and DGM was used for description of permeation process.

EXPERIMENTAL

Two porous catalysts in the form of cylindrical pellets were used: industrial hydrogenation catalyst Cherox 42-00 with monodisperse pore structure (Chemopetrol Litvínov, Czech Republic; height × diameter = 4.9 nm × 5.0 mm) and laboratory prepared α-alumina, A5 (based on boehmite from Pural SB, Condea Chemie, Germany) with bidisperse pore structure (height × diameter = 3.45 nm × 3.45 mm).

Four nonadsorbable gases (argon, helium, hydrogen, nitrogen; 99.9 % purity) were selected for transport measurements. Thus, the surface transport of adsorbed gases was absent.

Catalysts were characterized by two standard textural-analysis methods: *mercury porosimetry* (AutoPore 9200, Micromeritics, USA) and *physical adsorption of nitrogen* (ASAP2010M, Micromeritics, USA).

Two nonstandard transport processes (counter-current isobaric ternary diffusion and permeation of simple gases) were chosen for obtaining pore-structure transport characteristics. MTPM was used for evaluation of transport parameters.

The modified Wicke—Kallenbach cell developed in our laboratory [7, 8] was used for measurement of *isobaric counter-current ternary diffusion.* Fig. 1 shows schematically the diffusion set-up including the modified Wicke—Kallenbach cell. G1—3 are sources of all used gases (H_2, He, N_2, Ar); FMC are flow-meter controllers; D is the diffusion cell; O1—2 are gas outlets; V1—3 are valves; B is a calibrated glass burette with soap film. The diffusion cell contains a metallic disc with cylindrical holes into which the porous pellets are mounted. The nonporous rubber holds pellets in metallic disc. Volumes of cell compartments are approximately 150 cm^3

Measurement procedure: A mixture of two gases "1" and "2" flows through the bottom cell and another gas "3" flows through the upper cell compartment (flow-rates of gases in both cells are 150 cm^3 min^{-1}). Valves V1 and V3 are closed and valve V2 opened at the same time. Movement of the soap film in the burette follows the net diffusion flux. The net volumetric diffusion flux, V (cm^3 s^{-1}), gradually decreased with the increase of the gas "3" concentration in the bottom cell compartment. Net volumetric diffusion flux is determined from the slope at zero time of the $V(t)$ dependence.

Data evaluation: The evaluation of model parameters by nonlinear fitting of experimental net diffusion

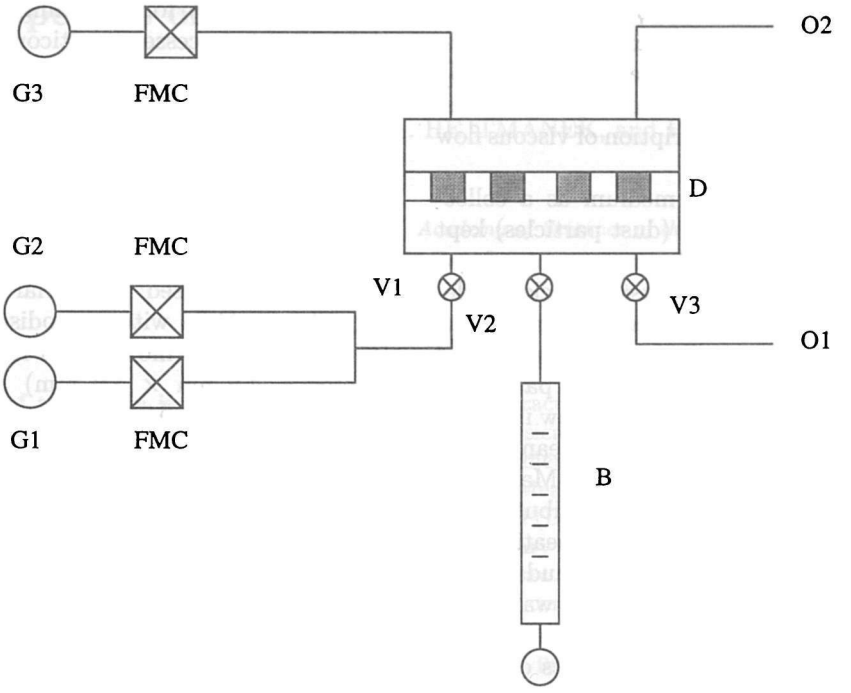

Fig. 1. Scheme of diffusion cell set-up.

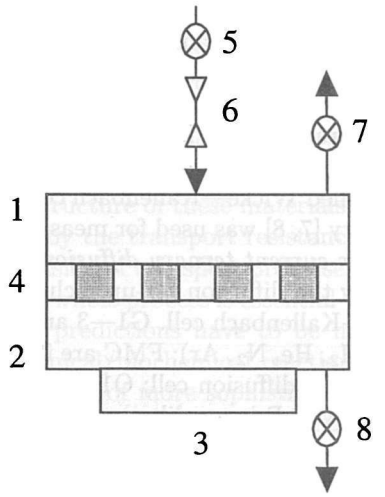

Fig. 2. Scheme of the permeation cell. *1.* Flow-through cell compartment, *2.* closed cell compartment, *3.* pressure transducer, *4.* metallic disc with pellets mounted into cylindrical holes, *5.* gas inlet valve, *6.* capillary, *7*, *8.* connection to vacuum pump.

flux densities to theory requires solution of a set of coupled ordinary differential equations which describe diffusion in porous solids according to MTPM (integration of differential equations with splitted boundary conditions).

Permeation (gas transport caused by pressure gradient) of simple gases is the second nonstandard process used for obtaining pore-structure transport characteristics. Permeation cell is shown in Fig. 2. It is divided by metallic disc with cylindrical pellets (about 15) into two parts. Volumes of parts are approximately 150 cm^3 The nonporous rubber holds pellets in metallic disc. The upper compartment of the cell is filled by one of the inert gas through a capillary (with known length and diameter) to prevent undesirable pressure shocks. Pressure is measured in lower cell compartment by an absolute pressure transducer (range 0—101 kPa, Omega Engineering, USA). Computer controls the whole measurement.

Measurement procedure: Both cell chambers are evacuated to the same pressure. Then the upper cell compartment is filled with the gas to the required pressure (approximately 101 kPa). This pressure step starts the permeation process in the porous material; the progress is followed by monitoring the pressure increase in the lower cell compartment. The time of gas filling is negligible in comparison with the length of the pressure response.

Data evaluation: Model parameters were obtained by fitting of experimental time dependences of pressure in the lower cell compartment to theory. Obtaining of theoretical time—pressure courses represents integration of mass balance (partial differential equation, or, assuming pseudo-steady state, ordinary differential equation).

All diffusion and permeation measurements were performed at laboratory temperature and used catalysts were not pretreated before measurements.

RESULTS AND DISCUSSION

The *isobaric counter-current diffusion measurements* in the modified Wicke—Kallenbach cell employ

the validity of the Graham law which states that under isobaric conditions the ratio of diffusion molar flux densities of components 1 and 2 equals the square root of the inverse ratio of molar masses of the gases

$$N_1/N_2 = -(M_2/M_1)^{1/2} \tag{2}$$

It follows, then, that both diffusion flux densities, N_1 and N_2, can be determined from the easily measurable net diffusion flux density $N = N_1 + N_2$.

For a system with three gas components, arranged so that gases 1 and 2 are in the bottom compartment of the diffusion cell and gas 3 is in the upper compartment, the system of ordinary differential equations is solved for porous pellets with the length L. The situation is described by the following system of equations

$$\frac{\mathrm{d}y_j}{\mathrm{d}x} = -\frac{1}{c_T}\left[\frac{N_1}{D_i^k} + \sum_{j=1}^{3}\frac{y_jN_i - y_iN_j}{D_{ij}^m}\right] \quad i = 1,2 \tag{3}$$

$$\frac{\mathrm{d}N_i}{\mathrm{d}x} = 0 \quad i = 1,2 \quad y_3 = 1 - \sum_{j=1}^{2} y_j \tag{4}$$

$$N_3 = -\sum_{j=1}^{2} N_j\sqrt{\frac{M_j}{M_3}} \quad N = \sum_{j=1}^{3} N_j \tag{5}$$

with initial conditions

$$\begin{aligned} &\text{at } x = 0 \quad y_1 = y_1^{\circ};\ y_2 = y_2^{\circ};\ y_3 = 0 \\ &\text{at } x = L \quad y_1 = 0;\ y_2 = 0;\ y_3 = y_3^{\mathrm{L}} \end{aligned} \tag{6}$$

Here x is the geometric coordinate in the porous pellet, N_i are the molar flux densities of gas mixture components, N is the net diffusion flux density, M_i are molar masses of mixture components, and y_i are component mole fractions. Superscripts o and L denote the bottom and upper part of the cell, respectively.

In the applied experimental arrangement the stream of pure heavier gas, or gas mixture containing the heavier gas, passed through the upper compartment. The net volumetric diffusion fluxes for catalyst A5 with He in the bottom cell compartment and mixtures of Ar and H_2, or Ar and N_2, in the upper compartment, are shown in Fig. 3. The dependent variable is the mole fraction of Ar in the (Ar + H_2) or (Ar + N_2) binary gas mixture. As can be seen mixture composition in the bottom compartment influences significantly the net diffusion fluxes. In agreement with the Graham law, this is the more marked the more differ the molar masses of gases. This figure also illustrates the change of the net diffusion flux direction (which appears as sign change of the net diffusion flux density).

For the transport parameter optimization the sets of 66 data points for both catalysts were used. These sets included data for binary cases (pure gases in both compartments) and ternary cases (pure gas in one compartment and a binary mixture in the other compartment). In Fig. 4 the experimental net volumetric diffusion fluxes are compared with calculated values based on the optimum sets of transport parameters. It can be seen that experimental and calculated diffusion fluxes are in a good agreement and experimental error does not exceed 3 %. The optimum transport parameters for both catalysts are summarized in Table 1.

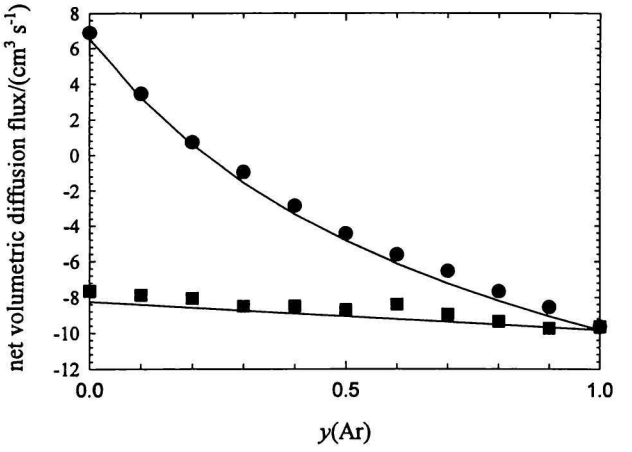

Fig. 3. Net volumetric diffusion fluxes; catalyst A5; ■ He/(Ar + N_2), ● He/(Ar + H_2).

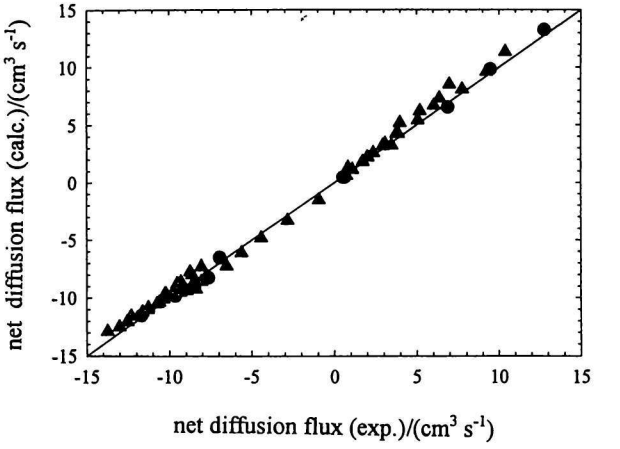

Fig. 4. Comparison of experimental and calculated net diffusion flux densities; catalyst A5; ▲ ternaries, ● binaries – pure gases.

Permeation: The permeation flux density, N, is described by the Darcy constitutive equation

$$N = -B\frac{\partial c}{\partial x} \tag{7}$$

where B is the effective permeation coefficient. Weber equation (*8*) describes the pressure dependence of

Table 1. Transport Parameters from Permeation and Diffusion Measurement

Porous solid	Permeation			Diffusion		
	$\langle r\rangle\,\psi$	$\langle r^2\rangle\,\psi$	$\langle r\rangle$	$\langle r\rangle\,\psi$	ψ	$\langle r\rangle$
	nm	nm^2	nm	nm		nm
A5	236	417732	1770	211	0.116	1818
Cherox 42-00	5.6	497	88	4.6	0.134	34

effective permeability coefficient B

$$B = D^{k}\frac{\omega + Kn}{1 + Kn} + B_0 RT\frac{c}{\mu} \qquad (8)$$

where D^{k} is the effective Knudsen diffusion coefficient defined as $2/3\langle r\rangle\psi(8RT/\pi M)^{1/2}$, B_0 is the Poiseuille parameter ($B_0 = \langle r^2\rangle\psi/8$), Kn is the Knudsen number at unit gas concentration (ratio of mean free-path length of the gas molecules and the pore diameter), and ω characterizes the slip at the pore wall.

For each catalyst and gas six experimental pressure dependences (each with more than 100 data points) were obtained with different initial pressure. Fig. 5 compares experimental results (points) with calculations (lines) for permeation of N_2 through Cherox 42-00. Both models (MTPM and DGM) gave nearly the same results. The optimum transport parameters are summarized in Table 1 together with transport parameters obtained from diffusion measurements. Radii of transport pores $\langle r\rangle$ were obtained as $\langle r\rangle^2\psi/\langle r\rangle\psi$ (for permeation) or as $\langle r\rangle\psi/\psi$ (for diffusion). It is evident from Table 1 that for A5 pellets the transport parameters $\langle r\rangle\psi$ from permeation and diffusion measurements are nearly the same (deviation about 10 %); the agreement for Cherox 42-00 is slightly worse (deviation about 20 %). Nearly the same results were obtained for calculated radii of mean transport pores, $\langle r\rangle$. For A5 pellets $\langle r\rangle = 1818$ nm (from diffusion) and 1770 nm (from permeation), *i.e.* an excellent agreement. For the Cherox 42-00 catalyst the agreement is less satisfactory.

Textural properties of both tested porous solids were determined by *physical adsorption of nitrogen* and *mercury porosimetry*, too. Pore-size distributions of catalysts obtained from physical adsorption of nitrogen (BJH algorithm) and from mercury porosimetry are compared with mean transport pore radii ($\langle r_d\rangle$ – diffusion, $\langle r_p\rangle$ – permeation) in Fig. 6. It is seen that the A5 pellets have bidisperse pore structure with maxima at 290 nm and 2070 nm. The mean transport pore radii are slightly smaller than the macropore peak of the pore-size distribution. Hence, the transport of gases passes mainly through the wider pores. For catalyst Cherox 42-00 the maximum of pore radii determined by the BJH algorithm is about 30 nm lower than from mercury porosimetry. The mean transport pore radius from diffusion measurement is

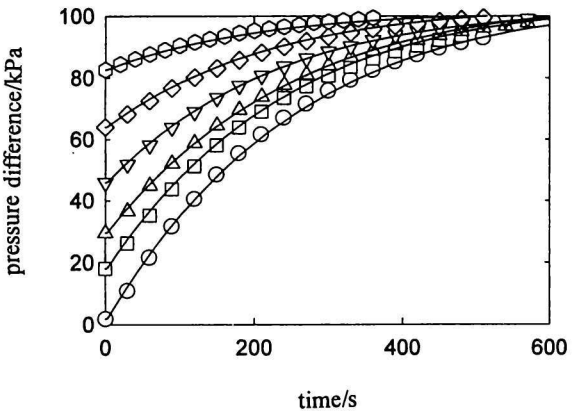

Fig. 5. Comparison of pressure difference for N_2 permeation in Cherox 42-00; points – experimental, line – calculated; initial pressure: ○ 1.88 kPa, □ 18.09 kPa, △ 29.48 kPa, ▽ 45.92 kPa, ◇ 64.01 kPa, ○ 82.61 kPa.

in a good agreement with maximum of pore radii determined by the BJH algorithm and the mean transport pore radius from permeation measurement is in a good agreement with the position of macropores determined by mercury porosimetry. But the deviation is not too significant.

CONCLUSION

Textural properties of two porous solids with different pore-size distributions were determined by two standard methods: physical adsorption of nitrogen and mercury porosimetry. The same porous solids were characterized by measurements of isobaric countercurrent diffusion and permeation of gases. MTPM and DGM were used for evaluation of transport parameters, which characterize textural properties in relation to gas transport. Transport parameters obtained from both nonstandard processes are in a good agreement. Mean transport pore radii from nonstandard processes and maxima of pore-size distributions from standard methods are similar for monodisperse pore structures; for solids with bidisperse pore-size distributions this difference is significant. It was confirmed that gas transport occurs mainly through wider pores. With respect to the complicated structure of porous catalysts it is hardly possible to use information on textural properties obtained from the two applied stan-

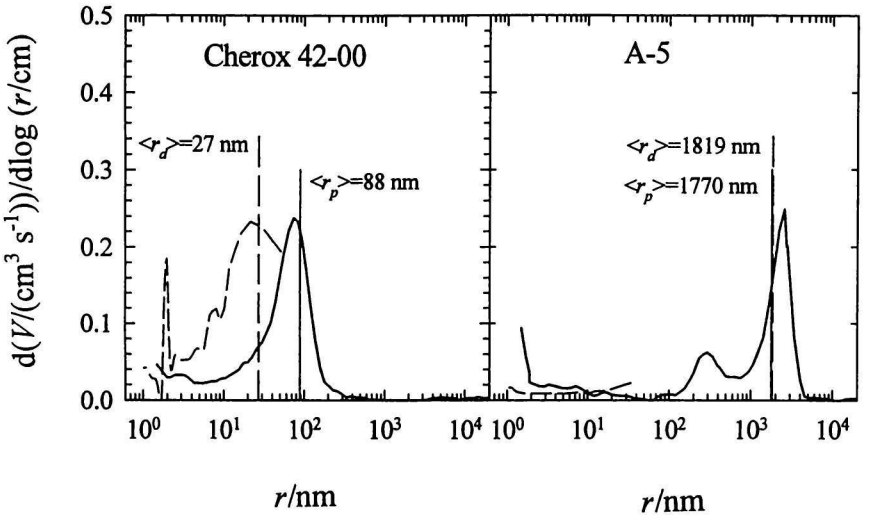

Fig. 6. Pore-size distributions. Mercury porosimetry – solid line, nitrogen physical adsorption – dashed line.

dard methods for prediction of gas transport in pores. It might be possible, however, to select another standard method, the physical principle of which is more similar to gas transport in pores. One can consider (for example) liquid-expansion permporometry. This method is based, among other, on the Washburn permeation equation for individual groups of pores.

SYMBOLS

B	effective permeability coefficient	$cm^2\ s^{-1}$
D^k	effective Knudsen diffusion coefficient	$cm^2\ s^{-1}$
D^m_{ij}	bulk diffusivity of pair i—j	$cm^2\ s^{-1}$
Di_j	Knudsen diffusivity of component i	$cm^2\ s^{-1}$
Kn	Knudsen number	
L	pellet length	cm
M_i	molar mass of component i	$g\ mol^{-1}$
N_i	molar flux density of component i	$mol\ cm^{-2}\ s^{-1}$
N	diffusion (permeation) flux density	$mol\ cm^{-2}\ s^{-1}$
p	pressure	kPa
q_t	tortuosity	
$\langle r\rangle$	mean transport pore radius	nm
$\langle r^2\rangle$	mean of squared transport pore radii	nm^2
R	gas constant	$J\ kmol^{-1}\ K^{-1}$
t	time	s
T	temperature	K
V	net volumetric diffusion flux	$cm^3\ s^{-1}$
x	length coordinate	
y_i	mole fraction of component	

Greek Letters

ε	porosity
ε_t	porosity of transport pores
μ	mixture viscosity
ψ	geometric transport parameters
ω	slip coefficient

Acknowledgements. The authors greatly appreciated financial support by the Grant Agency of the Academy of Sciences of the Czech Republic (A4072804, A4072915).

APPENDIX

The elements of matrix $\mathbf{H}(\boldsymbol{c})$ are defined as

$$h_{ii} = 1/D_i^k + (c_i\alpha_i/D_i^k) + \sum_{k=1}^{n}(c_k/(cD_{ik}))$$

$$h_{ij} = c_i\alpha_i/D_j^k - c_i/(cD_{ij}) \quad i \neq j$$

where D_{ij} is the effective bulk binary diffusion coefficient defined as $D_{ij} = \psi D_{ij}$ and D_i^k is the effective Knudsen diffusion coefficient

$$D_i^k = (2/3)\langle r\rangle\psi\sqrt{8RT/(\pi M_i)}$$

The bulk binary diffusion coefficients, D_{ij}, were taken from *Marrero* and *Mason* [9]. Differences between MTPM and DGM appear in the definition of parameter α_i:

For MTPM

$$\alpha_i = \left(1 - B_i/D_i^k - \sum_{k=1}^{n}(c_k(B_i - B_k)/(cD_{ik}))\right) \Big/ \Big/ \sum_{k=1}^{n}(c_kB_k/D_k^k)$$

Here B_i is the effective permeability coefficient of mixture component i [10]

$$B_i = D_i^k[(\omega\nu_i + Kn_i)/(1 + Kn_i)] + \langle r^2\rangle\psi p/(8\mu)$$

The numerical coefficient ω depends on the details of the wall-slip description ($\omega = 0.9, \pi/4, 3\pi/16$, *etc.*, see [10]); ν_i is the square root of the relative molar mass of the gas mixture component i

$$\nu_i = \sqrt{M_i / \sum_{j=1}^{n} \left(\frac{c_i}{c} M_j\right)}$$

μ is the gas mixture viscosity and Kn_i is the Knudsen number of component i (mean free-path length of component i/transport pore diameter).

For DGM

$$\alpha_i = -(\beta / D_i^{\mathrm{k}}) \Big/ \left(\sum_{k=1}^{n} c_k + \beta \sum_{k=1}^{n} (c_{\mathrm{k}} / D_k^{\mathrm{k}})\right)$$

$$\beta = \langle r^2 \rangle \psi p / (8\mu)$$

The mixture viscosity μ depends on the mixture composition and was calculated from the Reichenberg's formula [11].

REFERENCES

1. Schneider, P. and Gelbin, D., *Chem. Eng. Sci. 40,* 1093 (1985).
2. Fott, P., Petrini, G., and Schneider, P *Collect. Czech. Chem. Commun. 48*, 215 (1983).
3. Mason, E. A. and Malinauskas, A. P., Gas Transport in Porous Media, *The Dusty Gas Model.* Elsevier, Amsterdam, 1983.
4. Jackson, R., *Transport in Porous Catalysts.* Elsevier, Amsterdam, 1977.
5. Schneider, P., *Chem. Eng. Sci. 46*, 2376 (1991).
6. Novák, M., Ehrhardt, K., Klusáček, K., and Schneider, P., *Chem. Eng. Sci. 43*, 185 (1988).
7. Valuš, J. and Schneider, P., *Appl. Catal. 1*, 355 (1981).
8. Valuš, J. and Schneider, P., *Appl. Catal. 16*, 329 (1985).
9. Marrero, T. R. and Mason, E. A., *J. Phys. Chem. Ref. Data 1,* 3 (1972).
10. Weber, S., *Dan. Mat. Fys. Med. 28,* 1 (1954).
11. Reid, R. C., Prausnitz, J. M., and Poling, B. E., *The Properties of Gases and Liquids.* P. 404. McGraw-Hill, New York, 1988.